arXiv:1605.06073v3 [cond-mat.soft] 26 Mar 2017

Activity controls fragility: A Random First Order Transition Theory for an active glass

Saroj Kumar Nandi[1,*] and Nir S. Gov[2,†]

[1]*Department of Materials and Interfaces, The Weizmann Institute of Science, 234 Herzl Street, P.O. Box 26, Rehovot 7610001, Israel*

[2]*Department of Chemical Physics, Weizmann Institute of Science, Rehovot 7610001, Israel*

How activity modifies the properties of systems compared to their passive counterparts is an open question. Here, we extend a microscopic theory for the glassy dynamics of passive systems in their dense low-temperature limit, namely the Random First-Order Transition (RFOT) theory, to describe an active self-propelled particle system. We generalize and unify the findings of recent simulations and experiments on such systems and provide a number of testable predictions. Self-propulsion force, f_0, and persistence time, τ_p, characterize the activity of the constituent particles, and they were found in previous works to affect the system dynamics quite differently: f_0 inhibits glassiness, reducing the glass transition temperature and fragility of the system, whereas τ_p promotes glassiness and increases these parameters. Our theory explains these opposite effects of the two activity parameters, as arising due to their respective influence on the kinetic energy of the self-propelled particles that are caged within a dense glass.

Active systems, consisting of particles that can take up energy and do some mechanical work, can lead to an enriched and fascinating phenomenology compared to passive systems. As the particles consume energy and convert it into active motion, the system is driven far from equilibrium, and the kinetic and potential energies of the particles are modified compared to the passive system. Examples of active dense systems exists in biology, where the basic building blocks, from molecules to cells, constantly utilize chemical energy to perform different biological functions [1]. In a tissue, activity of cells is manifested through cell motility [2, 3], cell proliferation and apoptosis [4]. Recently artificial synthetic systems of self-propelled particles allow for a more systematic experimental investigation of the effects of activity. Examples include magnetic colloidal beads [5], catalytic Janus particles [6, 7], light activated colloidal swimmers [8], and vertically vibrated granular system [9, 10]. Simulations of model systems with different types of rules for the interactions and activity of the particles are also used to study the active motion in real systems [11–13]. These model numerical and experimental systems have only recently been studied in their dense limit [2, 3, 14–31]. These studies motivated attempts to extend the current descriptions of glassy phenomenology to the regime of active systems.

Mode-coupling theory (MCT) for glassy dynamics has been extended for dense active systems [14, 15, 25]. These theories, however, should be applicable within a limited regime since MCT itself fails at the high density (or low temperature) regime of a passive system where activated dynamics dominates [32, 33]. Self-propelled particle systems, where the particles are associated with an active self-propulsion force, f_0, and a persistence time, τ_p, are widely used to model many dense (glass-like) biological systems ranging from the motion inside cells [34, 35], to motion of cells in tissues [2, 3, 36], to large scale animal behavior. An analytic theoretical description of a self-propelled system in the dense glassy regime is important for our understanding of the behavior of such systems. In this work we extend random first order transition (RFOT) theory developed for glassy dynamics of passive systems [37–40] to a dense active system of self-propelled particles and show, through comparison with simulation data, that the theory captures the basic physics of such systems. We find that f_0 and τ_p affect the system in contrasting manners: while f_0 inhibits glassiness, and the transition points and fragility decreases quadratically with f_0, τ_p promotes glassiness, increasing the transition points and fragility with increasing τ_p.

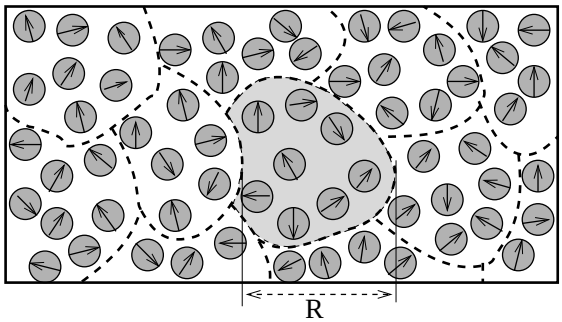

FIG. 1: Schematic picture of the mosaic concept of RFOT. The system consists of different regions of unique configurations of a typical length scale ℓ^*. Activity affects the system when ℓ^* decreases with f_0 and increases with τ_p. The dotted lines are schematic representation for a cluster of particles in the same state. Arrows on the particles indicate the instantaneous directions along which the self-propelled particles apply their motile force f_0, for a time scale of τ_p.

RFOT, developed by Kirkpatrick, Thirumalai and Wolynes is based on finite-dimensional extension of mean-field spin-glass models [37–39, 41, 42], and has been

remarkably successful [43–45] in describing a glassy system both above and below the regime where activated processes dominate the dynamics of the system. RFOT theory generalizes the theory of first-order crystallization transition to that of freezing to a disordered structure [39, 42], describing the system in terms of mosaics of local aperiodic structures (Fig. 1) and the mismatch energy at the interfaces of such mosaics [43–45]. Including activity within this basic RFOT picture presents a major challenge (see [46]) as it is unclear how does activity change the energy of the mosaic domains. We propose how to account for the additional energy due to activity, and thereby extend the RFOT theory to an active system.

Wolynes *et al* describe the activated reconfigurations of such mosaics through a mechanism similar to nucleation [37–39, 43, 47]. Let us consider a domain of volume v and length scale $R \sim v^{1/d}$, in d-dimension, as shown by the shaded region in Fig. 1. We can write the free energy gain of the system due to such reconfiguration as

$$\Delta F(R) = -\Omega_d R^d \Delta\tilde{f} + S_d R^\theta \bar{\gamma}(R), \tag{1}$$

where Ω_d is the volume and S_d, the surface of a region with unit radius in dimension d. The exponent is usually taken to be $\theta = d/2$, which is less than $d-1$ as expected for a smooth surface, to account for the rough fractal nature of the surface [38, 42]. For a passive system $\Delta\tilde{f} = T\Sigma(T)$, where $\Sigma(T)$ is the configurational entropy of the system at temperature T. We propose that the activity adds an additive term to this bulk term, and write: $\Delta\tilde{f} = T\Sigma(T) + \mathcal{F}_A$, where $\mathcal{F}_A$ is the contribution coming from activity. The second term in Eq. (1) is akin to a surface tension term and accounts for the mismatch of different states at the surface. We write $\bar{\gamma}(R) = \Upsilon_0(T)(1+\gamma_A)$, where Υ_0 gives the contribution for a passive system and γ_A gives the modification due to activity. This separation into passive and active parts is an approximation and may not always be possible, but for the systems of self-propelled particles, we are going to show, that this approximation yields excellent agreement with simulation data. Note that Υ_0 fluctuates even in a passive system [48] and γ_A can have additional contributions from localized heating or chemical reactions leading to Marangoni stresses in an active system [49] that we ignore here. As discussed in the Sup. Mat. [46], the modification of the surface energy due to activity turns out to be negligible and we ignore γ_A from now on. Minimizing Eq. (1) with respect to the domain size, we obtain

$$\ell^* = \left[\frac{\theta S_d \Upsilon_0(T)}{d\Omega_d T(\Sigma(T) + \mathcal{F}_A/T)}\right]^{1/(d-\theta)}. \tag{2}$$

This expression constitutes the central result for an active system. If the length scale R of the cavity is larger than ℓ^*, then the volume (first) term in Eq. (1) wins and the cavity lowers its energy through reconfiguration. In the other limit, the surface term wins and the state within the cavity remains the same. Thus, the system consists of mosaics of correlated states with a typical length scale ℓ^*. Note that this length-scale is different from dynamic length-scales associated with domains of correlated motion [3].

The Kauzmann temperature T_K is defined where configurational entropy $\Sigma(T_K)$ of the passive system vanishes [50]. Therefore close to but above T_K we can write $\Sigma(T) = \Delta C_p(T - T_K)/T_K$, where ΔC_p is the jump in specific heat from the liquid to the crystalline state [50]. We assume that the temperature-dependence of $\Upsilon_0(T)$ is linear: $\Upsilon_0(T) = \kappa T$, where κ is a constant [51]. The detailed T-dependence of $\Upsilon_0(T)$ doesn't change the qualitative results because the change in configurational entropy plays the major role in governing the dynamics [51]. Defining $D = c_d \kappa T_K/\Delta C_p$, where $c_d = \theta S_d/d\Omega_d$ and taking $\theta = d/2$, as has been advocated by Wolynes *et al* [39, 42], close to T_K we obtain

$$\ell^* = \left[\frac{D}{(T - T_K) + \frac{\mathcal{F}_A}{\Delta C_p}}\right]^{2/d}. \tag{3}$$

The relaxation dynamics of the system is characterized by the reconfiguration of a mosaic of length scale ℓ^*. The typical barrier height for the relaxation of the system is $\Delta(\ell^*) \sim \Delta_0 \ell^{*\psi}$, where Δ_0 is a T-dependent energy scale and ψ, an exponent. Then the relaxation time τ of the system is $\tau \sim \tau_0 \exp\left(\frac{\Delta_0 \ell^{*\psi}}{T}\right)$, where τ_0 is a microscopic time scale determined by the inter-particle interactions. Based on a nucleation type of argument, Wolynes *et al* showed that $\psi = \theta = d/2$ [38]. Following [38], we assume $\Delta_0 = \Upsilon_0 = \kappa T$ where κ is a constant and obtain (close to T_K)

$$\ln\left(\frac{\tau}{\tau_0}\right) = \frac{c_d \kappa^2 T_K}{\Delta C_p (T - T_K) + \mathcal{F}_A} = \frac{E}{(T - T_K) + \frac{\mathcal{F}_A}{\Delta C_p}} \tag{4}$$

where $E = c_d \kappa^2 T_K/\Delta C_p$. Thus, within the extended-RFOT for an active system, we need to obtain the activity-dependent parameter $\mathcal{F}_A$.

Let us now concentrate on the system of self-propelled particles [12, 13, 16, 18]. We consider the dynamics of one of the particles surrounded by all the other particles. In the dense regime we can approximate the caging effect of the other particles as a confining harmonic potential of strength k [52]. As $\mathcal{F}_A$ is an entropic contribution, we expect that it will be dominated by the kinetic energy of this confined particle due to activity, and we obtain

(Eqs. S1-S4)

$$\mathcal{F}_A = \frac{f_0^2 \tau_p}{4[\lambda(1+\tau_p\lambda) + \pi\tau_p^2\sqrt{k^3/8}]} \tag{5}$$

$$\approx \frac{\tilde{H} f_0^2}{(1+G\tau_p)} \tag{6}$$

where λ is the friction coefficient, and Eq. (6) is in the over-damped limit $\lambda\tau_p \gg 1$ and $\tilde{H}$ and G are two constants determined by the microscopic properties of the system [46, 52]. A similar result was also obtained in [18] in the context of the Lindemann criterion. Note that the active kinetic energy is quadratic in the active force, as expected, while the persistence time causes it to decrease. This is in contrast to the role of τ_p for free particles [53] and arises due to the particles spending more time immobile against the confining potential for larger persistence times. This effect of τ_p is similar to the activity-induced aggregation of self-propelled particles in dilute systems [28, 54, 55], and near boundaries [56, 57]. τ_p introduces an effective attractive potential (though transient), making the particles less mobile [23, 24, 55]. From Eqs. (3) and (4) we obtain [in the over-damped limit, Eq. (6)]

$$\ell^* = \left[\frac{D}{(T-T_K) + \frac{Hf_0^2}{1+G\tau_p}}\right]^{2/d} \tag{7}$$

$$\ln\left[\frac{\tau}{\tau_0}\right] = \frac{E}{(T-T_K) + \frac{Hf_0^2}{1+G\tau_p}}. \tag{8}$$

where $H = \tilde{H}/\Delta C_p$. Eq. (7) shows that f_0 decreases the effective Kauzmann temperature $T_K^{eff} = T_K - Hf_0^2/(1+G\tau_p)$, defined as the temperature when ℓ^* and τ diverge, whereas τ_p increases it. In other words, at a fixed τ_p, as we increase f_0 the system shows glassy behavior at lower T compared to the corresponding passive system, i.e., f_0 suppresses glassiness as has been observed in many systems [15, 16, 18, 19, 21]. On the other hand, at a fixed f_0, if we increase τ_p the system shows glassy behavior at higher T, i.e., τ_p promotes glassiness, which has also been observed in simulations [16, 26]. These opposite effects of the propulsion force and the persistence time on the glass transition in active glasses remained an open puzzle, which is naturally explained using our model.

We now compare quantitatively our model's predictions of the effects of activity on ℓ^* and τ to simulation results. We begin with a fixed τ_p, when activity is controlled through f_0. We plot ℓ^* and τ as a function of T in Fig. 2(a) and (b) respectively [46]. We see that at a given T, ℓ^* as well as τ decrease as we increase f_0. We define the glass transition temperature T_g when the relaxation time of the system increases beyond the threshold value of $\tau/\tau_0 = 10^6$. From Eq. (8) we see that T_g gets modified due to activity as $T_g = E/(6\ln 10) + T_K - Hf_0^2/(1+G\tau_p)$, similar to T_K^{eff}. Using this definition we compare our theory with molecular dynamics simulation data of a Kob-Andersen binary mixture of an active system [18], by rewriting Eq. (8) as

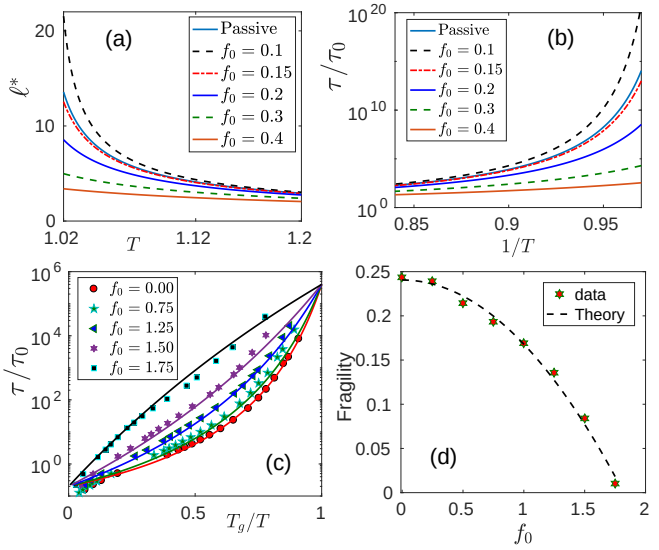

FIG. 2: Results when the self-propulsion force f_0 is the control parameter. (a) Behavior of typical length scale ℓ^* of the mosaics of an active system as a function of temperature T at constant persistence time $\tau_p = 0.02$, according to Eq. (7). At all T, ℓ^* decreases with increasing self-propulsion, f_0. (b) Relaxation time τ of the active system as a function of $1/T$ with $\tau_p = 0.02$, according to Eq. (8). As f_0 increases, growth of τ/τ_0 becomes slower and the system relaxes faster at a certain T. (c) Angell plot for τ as a function of T_g/T. The data are from Ref. [18] and the lines are our theoretical calculations using Eq. (9) (see [46]). As activity increases, the behavior of τ becomes closer to Arrhenius law, making the system a stronger glass former. (d) Behavior of fragility as a function of activity. Data taken from Ref. [18] and the line is our theoretical calculation, Eq. (10).

$$\ln\left(\frac{\tau}{\tau_0}\right) = \frac{E}{(T-T_K) + \frac{f_0^2}{\Lambda}} \tag{9}$$

where Λ is a constant since τ_p is kept fixed. We obtain the values of the constant parameters by fitting our analytical expression to one particular data set, at $f_0 = 1.50$, and obtain $\tau_0 = 5.0$, $T_K = 0.2$, $E = 1.05$ and $\Lambda = 14.0$ (note that we can only obtain these parameters up to a constant factor). In Fig. 2(c) we show the Angell plot [58] where the symbols are data taken from [18] and the lines are the theoretical predictions [Eq. (9)]. We emphasize here that the theoretical lines are *not* individual fits to the simulation data, since all the plots of Eq. (9) use the same constant parameter values obtained from one initial fit. We obtain the fragility parameter m of the system, defined as $m = -T\partial\ln(\tau/\tau_0)/\partial T\big|_{T=T_g}$ [43], which becomes

$$m = \frac{(6\ln 10)^2}{E}\left[\frac{E}{6\ln 10} + T_K - \frac{Hf_0^2}{1+G\tau_p}\right]. \tag{10}$$

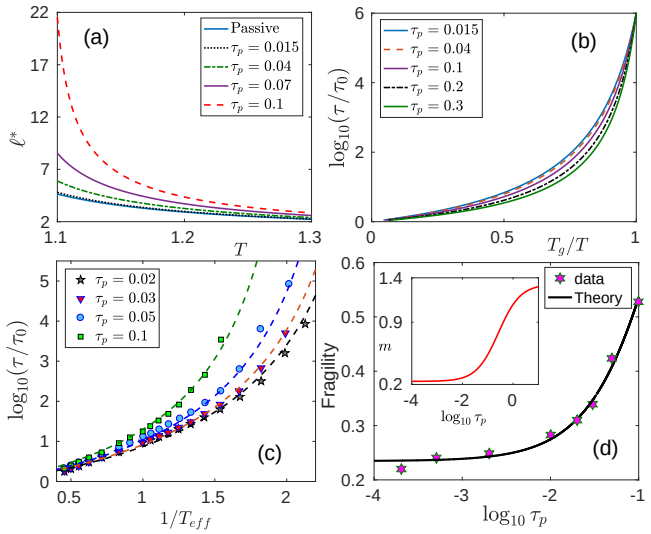

FIG. 3: Results when activity is controlled by varying the persistence time τ_p. (a) ℓ^* as a function of T for different τ_p with $f_0 = 0.1$, using Eq. (7). (b) We define T_g when τ/τ_0 becomes 10^6 and plot $\log(\tau/\tau_0)$ as a function of T_g/T for $f_0 = 0.8$, using Eq. (8). As τ_p increases, the curves depart further from the Arrhenius behavior, which means the system becomes more fragile with increasing τ_p. (c) Relaxation time of the system as a function of $1/T_{eff}$ at different τ_p. We compare our theoretical results for τ, with the simulation data of Ref. [26]. As the system dynamics in [26] comes from activity alone, τ_0 becomes a function of τ_p when τ_p dominates the dynamics and we obtain $\tau_0 = 0.0615$, 0.0807, 0.0992 and 0.1863 for $\tau_p = 0.02$, 0.03, 0.05 and 0.1 respectively (see [46]). (d) We expect the fragility to increase roughly linearly with τ_p from our theory [Eq. (10)], and this matches quite well with the simulation data of [26]. **Inset:** Our theory predicts that the fragility saturates at large τ_p.

For fixed τ_p we can therefore write: $m = c_1 - c_2 f_0^2$, where c_1 and c_2 are two constants. We fit this form to the simulation data [18] as shown in Fig. 2(d) and find that the trend is well-predicted by theory, as $c_1/c_2 = 3.8$ and 3.7 using the constants obtained in Fig. 2(c) and from a direct fit respectively. As f_0 increases, the behavior of τ becomes closer to Arrhenius law implying that the system becomes a stronger glass former according to the classification of Angell [58]. Thus, if τ_p is fixed and activity is controlled through f_0, the system becomes a stronger glass former with increasing activity.

We next examine systems where the particles have a constant f_0 and activity is controlled through changing τ_p. We set f_0 constant and show the behavior of ℓ^* as a function of T as we increase τ_p (Fig. 3a). At any value of T as we increase τ_p, we see ℓ^* increases monotonically. Thus, τ_p promotes glassy behavior in the active system, as found in [26]. To look at the behavior of τ as a function of τ_p, we show the Angell plot [58] (Fig. 3b). We find that the curves depart further from the Arrhenius behavior as τ_p increases, which means fragility increases with τ_p. From our theory, we obtain that the effective Kauzmann temperature, T_K^{eff}, glass transition temperature, T_g, and fragility, m [Eq. (10)], all increase with τ_p when f_0 remains constant. For a quantitative comparison of our theory with simulation data of [26], we write Eq. (4) as (see Eq. (S13) in [46]): $\ln\tau = \ln\tau_0 + \tilde{E}/[-\tilde{T}_K + T_{eff}/(1+\tilde{A}\tau_p)]$, where $T_{eff} \sim f_0^2\tau_p$ and we use Eq. (5) in the regime of small τ_p (Eq. (S11) in [46]). Since the dynamics of the system in [26] is a result of activity alone, τ_0 becomes a function of τ_p, and we fit a value of τ_0 for each value of τ_p, as was done in [26] (see Fig. S2 in [46]). Note that τ_0 determines only the large T_{eff} limit, while our model gives precise prediction for the behavior in the limit of small T_{eff}, approaching the glassy regime. We compare our theoretical results to the data of [26] in Fig. 3(c) using: $\tilde{E} = 1.255$, $\tilde{T}_K = 0.305$ and $\tilde{A} = 3.801$. We also obtained the data for fragility m from Fig. 11(b) of [26] and fit it with our theoretical prediction [Eq. (10)]: $m = a - b/(1+\tilde{A}\tau_p)$, with $a = 1.328$ and $b = 1.093$ (Fig. 3d). Our theory predicts that m saturates at large τ_p (Fig. 3(d) inset). Irrespective of the detailed behavior, the system becomes more fragile as τ_p increases, opposite to the behavior for increasing f_0.

What are the implications of our results for a real biological system? Activity of the individual elements in these systems can be controlled externally, for example through the regulation of ATP in the case of cells. However, it is not clear how such external controls affect the activity parameters, f_0 or τ_p of the active elements. Our results provide a route to classify the effects of the manipulation of the activity. Ref. [29] shows that the cytoplasm of cells behaves as a strong glass former material, and when ATP is depleted the system becomes more fragile [30]. Cytoplasms of cells consist of many molecular motors and higher ATP concentration will drive more motors to be in the active state, which will increase $\tilde{H}$ (Eq. (S3) in [46]). This is effectively increasing f_0^2 [Eq. (5)] and therefore according to our model this suggests that higher ATP decreases the fragility, driving the system towards a strong glass former.

Beyond biological systems, active glasses present an open challenge for physics theory, and the main advances in this field relied so far on numerical simulations. Refs. [18] and [26] have produced data indicating the opposite roles of the active parameters. Our model provides analytic expressions that give excellent description of available numerical simulation results, and resolves the seeming contradiction between the effects of f_0 and τ_p. We trace this behavior to the kinetic energy of a caged active particle, which makes our results qualitatively independent of the exact form of the inter-particle interaction potential. The competition between the increased mobility and increased particle aggregation, which are both generated by activity, leads to fascinating physics and may play important roles in different biological processes

in living organisms.

We would like to thank Sriram Ramaswamy and Peter G. Wolynes for important suggestions and discussions.

* Electronic address: saroj.nandi@weizmann.ac.il
† Electronic address: nir.gov@weizmann.ac.il

[1] J. Prost, F. Jülicher, and J. F. Joanny, Nat. Phys. **11**, 111 (2015).
[2] T. E. Angelini, E. Hannezo, X. Trepat, M. Marquez, J. J. Fredberg, and D. A. Weitz, Proc. Natl. Acad. Sci. (USA) **108**, 4717 (2011).
[3] S. Garcia, E. Hannezo, J. Elgeti, J. F. Joanny, P. Silberzan, and N. S. Gov, Proc. Natl. Acad. Sci. (USA) **112**, 15314 (2015).
[4] J. Ranft, M. Basan, J. Elgeti, J. F. Joanny, J. Prost, and F. Jülicher, Proc. Natl. Acad. Sci. USA **107**, 20863 (2010).
[5] R. Dreyfus, J. Baudry, M. L. Roper, M. Fermigier, H. A. Stone, and J. Bibette, Nature **437**, 862 (2005).
[6] J. R. Howse, R. A. L. Jones, A. J. Ryan, T. Gough, R. Vafabakhsh, and R. Golestanian, Phys. Rev. Lett. **99**, 048102 (2007).
[7] J. Palacci, C. Cottin-Bizonne, C. Ybert, and L. Bocquet, Phys. Rev. Lett. **105**, 088304 (2010).
[8] J. Palacci, S. Sacanna, A. P. S. D. J. Pine, and P. M. Chaikin, Science **339**, 936 (2013).
[9] N. Kumar, H. Soni, S. Ramaswamy, and A. K. Sood, Nat. Comm. **5**, 4688 (2014).
[10] O. Dauchot, G. Marty, and G. Biroli, Phys. Rev. Lett. **95**, 265701 (2005).
[11] T. Vicsek, A. Czirók, E. Ben-Jacob, I. Cohen, and O. Shochet, Phys. Rev. Lett. **75**, 1226 (1995).
[12] S. Ramaswamy, Annu. Rev. Condens. Matter Phys. **1**, 323 (2010)
[13] M. C. Marchetti, J. F. Joanny, S. Ramaswamy, T. B. Liverpool, J. Prost, M. Rao, and R. A. Simha, Rev. Mod. Phys. **85**, 1143 (2013).
[14] T. Kranz, M. Sperl, and A. Zippelius, Phys. Rev. Lett. **104**, 225701 (2010).
[15] L. Berthier and J. Kurchan, Nat. Phys. **9**, 310 (2013).
[16] R. Ni, M. A. C. Stuart, and M. Dijkstra, Nat. Commun **4**, 2704 (2013).
[17] O. Chepizhko and F. Peruani, Phys. Rev. Lett. **111**, 160604 (2013).
[18] R. Mandal, P. J. BHuyan, M. Rao, and C. Dasgupta, Soft Matter **12**, 6268 (2016).
[19] L. Berthier, Phys. Rev. Lett. **112**, 220602 (2014).
[20] D. Bi, J. H. Lopez, J. M. Schwarz, and M. L. Manning, Nat. Phys. **11**, 1074 (2015).
[21] B. R. Parry, I. V. Surovtsev, M. T. Cabenn, C. S. O'Hern, E. R. Dufresne, and C. Jacobs-Wagner, Cell **156**, 183 (2014).
[22] R. Ni, M. A. C. Stuart, M. Dijkstra, and P. G. Bolhuis, Soft Matter **10**, 6609 (2014).
[23] D. Levis and L. Berthier, Europhys. Lett. **111**, 60006 (2015).
[24] F. Ginot, I. Theurkauff, D. Levis, C. Ybert, L. Bocquet, L. Berthier, and C. Cottin-Bizonne, Phys. Rev. X **5**, 011004 (2015).
[25] G. Szamel, Phys. Rev. E **93**, 012603 (2016).
[26] E. Flenner, G. Szamel, and L. Berthier, Soft Matter **12**, 7136 (2016).
[27] C. Bechinger, R. D. Leonardo, H. Löwen, C. Reichhardt, G. Volpe, and G. Volpe, Rev. Mod. Phys. **88**, 045006 (2016).
[28] G. S. Redner, C. G. Wagner, A. Baskaran, and M. F. Hagan, Phys. Rev. Lett. **117**, 148002 (2016).
[29] E. H. Zhou, X. Trepat, C. Y. Park, G. Lenormand, M. N. Oliver, S. M. Mijailovich, C. Hardin, D. A. Weitz, J. P. Butler, and J. J. Fredberg, Proc. Natl. Acad. Sci. (USA) **106**, 10632 (2009).
[30] M. Sadati, A. Nourhani, J. J. Fredberg, and N. T. Qazvini, WIREs Syst. Biol. Med. **6**, 137 (2014).
[31] N. Gravish, G. Gold, A. Zangwill, M. A. D. Goodisman, and D. I. Goldman, Soft Matter **11**, 6552 (2015).
[32] L. Berthier and G. Biroli, Rev. Mod. Phys. **83**, 587 (2011).
[33] M. K. Nandi, A. Banerjee, S. Sengupta, S. Sastry, and S. M. Bhattacharyya, J. Chem. Phys. **143**, 174504 (2015).
[34] É. Fodor, M. Guo, N. S. Gov, P. Visco, D. A. Weitz, and F. van Wijland, Europhys. Lett. **110**, 48005 (2015).
[35] W. Ahmed, E. Fodor, M. Almonacid, M. Bussonnier, M.-H. Verlhac, N. Gov, P. Visco, and F. van Wijland Timo Betz, Biophys. J. **110**, 198a (2016).
[36] D. Bi, X. Yang, M. C. Marchetti, and M. L. Manning, Phys. Rev. X **6**, 021011 (2016).
[37] T. R. Kirkpatrick and P. G. Wolynes, Phys. Rev. A **35**, 3072 (1987).
[38] T. R. Kirkpatrick, D. Thirumalai, and P. G. Wolynes, Phys. Rev. A **40**, 1045 (1989).
[39] V. Lubchenko and P. G. Wolynes, Annu. Rev. Phys. Chem. **58**, 235 (2007).
[40] J. P. Bouchaud and G. Biroli, J. Chem. Phys. **121**, 7347 (2004).
[41] G. Biroli and J. P. Bouchaud, in *Structural Glasses and Supercooled Liquids: Theory, Experiment, and Applications*, edited by P. G. Wolynes and V. Lubchenko (John Wiley and Sons, Inc., Hoboken, NJ, USA, 2012).
[42] T. R. Kirkpatrick and D. Thirumalai, Rev. Mod. Phys. **87**, 183 (2015).
[43] X. Xia and P. G. Wolynes, Proc. Natl. Acad. Sci. USA **97**, 2990 (2000).
[44] A. Wisitsorasak and P. G. Wolynes, Proc. Natl. Acad. Sci. USA **109**, 16068 (2012).
[45] P. G. Wolynes, Proc. Natl. Acad. Sci. USA **106**, 1353 (2009).
[46] See Sup. Mat.
[47] V. Lubchenko and P. Rabochiy, J. Phys. Chem. B **118**, 13744 (2014).
[48] G. Biroli, J. P. Bouchaud, A. Cavagna, T. S. Grigera, and P. Verrocchio, Nat. Phys. **4**, 771 (2008).
[49] A. Domínguez, P. Malgaretti, M. Popescu, and S. Dietrich, Phys. Rev. Lett. **116**, 078301 (2016).
[50] W. Kauzmann, Chem. Rev. **43**, 219 (1948).
[51] P. G. Wolynes and V. Lubchenko, *Structural Glasses and Supercooled Liquids* (John Wiley and Sons, Inc., Hoboken, New Jersey, 2012).
[52] E. Ben-Isaac, É. Fodor, P. Visco, F. van Wijland, and N. S. Gov, Phys. Rev. E **92**, 012716 (2015).
[53] E. Ben-Isaac, Y. Park, G. Popescu, F. L. H. Brown, N. S. Gov, and Y. Shokef, Phys. Rev. Lett. **106**, 238103 (2011).
[54] D. Levis and L. Berthier, Phys. Rev. E **89**, 062301 (2014).

[55] M. F. Hagan and A. Baskaran, Curr. Opinion in Cell Biol. **38**, 74 (2016).
[56] H. H. Wensink and H. Löwen, Phys. Rev. E **78**, 031409 (2008).
[57] J. Elgeti and G. Gompper, Europhys. Lett. **101**, 48003 (2013).
[58] C. A. Angell, J. Non-Cryst. Solids **131-133**, 13 (1991).

Supplemental Material: Activity controls fragility: A Random First Order Transition Theory for an active glass

Systems of self-propelled particles, associated with an active self-propulsion force, f_0, and a persistence time, τ_p, are good representations for a large class of systems, for example, a tissue where the cells follow a directed motion driven by ATP [1–3], an ensemble of animals such as ants, fishes or birds [4, 5] or the experimental system of vertically vibrated polar rods [6, 7]. Ref. [2] provides an elegant hydrodynamic description of a normal visco-elastic tissue where the cells undergo diffusive random motion through the stochasticity of cell-division and apoptosis. Understanding the glassy dynamics under activity is important since the viscosity inside a cell and in a tissue are quite large compared to the viscosity of water. These systems are sometimes modeled as Newtonian liquids [4] and as elastic materials [8], both leading to important results. The reason is, possibly, that these systems act as glassy systems. However, in these systems, it is not obvious how the internal activity is affected by changes in the concentration of ATP (adenosine tri-phosphate) or some other chemical substances. A detailed understanding of a self-propelled system in the dense regime is important to elucidate how the key parameters affect the system and explain the behavior of such systems in general.

Challenges in extending Random First Order Transition (RFOT) Theory for an active system

Including activity within the basic RFOT picture presents a number of difficulties:

- Active systems are inevitably out of equilibrium and it is not clear how far an extension of a theory that is based on equilibrium thermodynamics is going to be valid.
- As the term 'active system' describes a diverse class of systems, where activity plays significantly different roles in different systems, a unified description is unrealistic at present.
- Configurational entropy, $\Sigma(T)$, and the surface mismatch energy play the major roles within RFOT phenomenology and the precise nature how activity affects these quantities is not known (however, see [9] for results on configurational entropy of active systems in the dilute limit, i.e., away from the glassy regime).
- It is not clear if the basic mosaic picture will survive under activity.

Here we show that, although there is no direct proof, there already exists experimental and simulation results that support the validity of basic RFOT phenomenology in an active system. Our work follows the spirit that a thermodynamic-like description of the system still exists even in the presence of active noise and different thermodynamic quantities consist of active and passive contributions [10–16]. In certain cases, time-reversal symmetry is satisfied [17] and one can describe the system in terms of an effective-temperature (T_{eff}) [9, 18–24]. However, the limit of applicability of this concept is currently being spiritedly debated [17, 25].

The basic building block of RFOT theory is the existence of local structures, known as mosaics of different states, as schematically shown in Fig. 1. Does this scenario of mosaics for equilibrium glasses still hold for an active system? Ref. [26] looks at the collective cell migration within a confluent epithelial cell sheet and finds a remarkable similarity of the dynamics with the dynamics of a glassy system approaching the glass-transition. They find that groups of cells move in clusters whose length scale increase as density of cells increases. In the cellular motion within a monolayer, Ref. [3] also finds similar clusters within which the cells move cooperatively. Although, these findings are not proof of the mosaic scenario, they certainly support it. A large number of recent studies [27–29] show that the active glass has remarkable similarity, albeit modified by activity, with the equilibrium glasses. Thus, there is no *a-priori* reason to expect the break down of the mosaic scenario. We assume that the mosaic picture of RFOT survives under activity and justify our assumption through comparison of our theoretical results with simulation data on two different types of self-propelled particle systems [28, 30] as shown in Figs. 2, 3.

Active contribution to mosaic reconfiguration energy

Let us consider the dynamics of an active particle within a certain mosaic. For simplicity, we consider a one-dimensional picture though the arguments can be easily extended to higher dimensions. In the dense regime that we are interested in, the particle will be surrounded (caged) by the other particles, reducing its mobility. We

can approximate the effect of the other particles through a harmonic potential $U(x) = kx^2/2$, which is generally dependent on temperature and density. Then we can write down the Langevin equation describing the particle velocity v as [31]

$$\dot{v} = -\lambda v + f_a + f_T - \frac{\partial U(x)}{\partial x}, \tag{S1}$$

where λ is an effective friction coefficient, f_T, the thermal noise with zero mean and $\langle f_T(t) f_T(t')\rangle = 2\lambda T\delta(t-t')$ and the active noise f_a that arises as the particles exert a constant force in a random direction for a time-period of τ_p.

The active noise in [31] was modeled as combination of N_m motors each of which can turn on randomly as a Poisson process after an average waiting time τ_w. The probability of a particular motor to be turned on becomes $p_{on} = \tau_p/(\tau_w + \tau_p)$. For the particular model we have considered, we will have $N_m = 1$, $\tau_w = 0$ and therefore, $p_{on} = 1$. Since we are interested in the entropic contribution coming from the active noise, we need to look at the kinetic part of the active energy. Following [31] we obtain

$$\langle v^2\rangle = \frac{N_m p_{on} f_0^2}{2\pi}\int_0^\infty \frac{\omega^2}{(\omega^2-k)^2+(\omega\lambda)^2}\frac{\tau_p}{1+(\omega\tau_p)^2}\mathrm{d}\omega. \tag{S2}$$

(See Eq. (C1) in [31], note that τ_p is $\Delta\tau$ in their notation). In the glassy regime we are interested in the over-damped limit and obtain

$$\langle v^2\rangle = \frac{N_m p_{on} f_0^2 \tau_p}{4[\lambda(1+\tau_p\lambda) + \pi\tau_p^2\sqrt{k^3/8}]} \tag{S3}$$

Taking the limit $\tau_p\lambda \gg 1$, we obtain

$$\langle v^2\rangle = \frac{\tilde{H} f_0^2}{1+G\tau_p} \tag{S4}$$

where $\tilde{H} = N_m p_{on}/4\lambda^2$ and $G = \sqrt{k^3/8}/\lambda^2$. Deep in the glassy regime, we assume k to be independent of temperature and G is a constant. Note that p_{on} and hence $\tilde{H}$ can depend on τ_p when $\tau_w \neq 0$. Ref. [30] also obtained similar results modeling the effect of other particles as a caging potential.

Then, we obtain the modification to the entropy-driven reconfiguration energy, $\mathcal{F}_A \sim \tilde{H} f_0^2/(1+G\tau_p)$. We expect a similar form for γ_A as well. However, using different forms of $\gamma_A(v_0, \tau_p)$ to fit with the available simulation [28, 30] data, it seems that the modification to the surface energy term due to activity is sub-dominant and we neglected γ_A in the paper. The scenario is somewhat similar to the passive system where temperature-dependence of the surface energy term doesn't alter the qualitative behavior [32]. However, we note that it is not *a-priori* obvious why the activity-contribution to the surface energy term should be sub-dominant, and requires further investigation to establish its regime of validity. It is possible that such behavior is found only for the particular system we looked at and can not be generic [33]. We emphasize that the surface energy term $\bar{\gamma}(R)$ is different from the surface tension in a phase-separating active system where the surface tension may become negative [25].

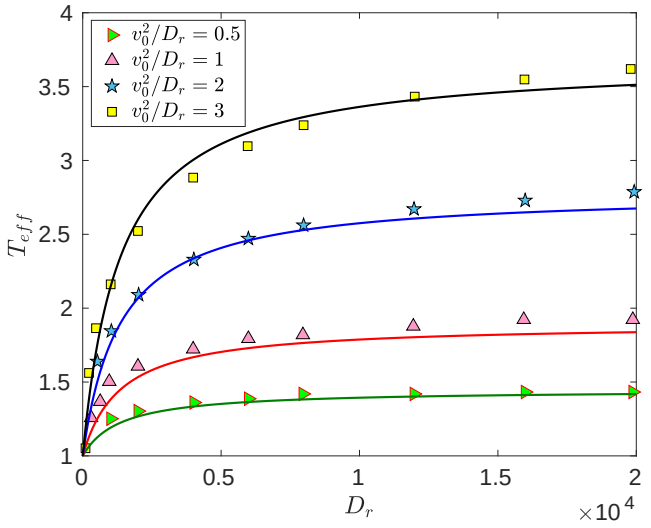

FIG. S1: We test the assumption of using Eq. (S3) as the modification to configurational entropy due to activity. Symbols are data obtained from Fig. 4(b) of [9] and solid lines are plots of Eq. (S5) with $A = 0.893951$ and $B = 1350.5$.

In a very nice recent work Ref. [9] shows that one can write down the non-equilibrium equivalent of configurational entropy through an effective temperature T_{eff}. Our calculation is similar in spirit although we assumed that T_{eff} is proportional to the kinetic energy of a single particle caged within a confining potential generated by all the other particles, as obtained in Eq. (S3). Here we test the validity of this assumption. Ref. [9] considers the coefficient of rotational Brownian motion, D_r, as a measure of persistence and $D_r \sim 1/\tau_p$. Using Eq. (S3) we obtain T_{eff} in terms of D_r and v_0, the self-propulsion velocity, as

$$T_{eff} = 1 + \frac{A(v_0^2/D_r)D_r}{B + D_r} \tag{S5}$$

where we have set temperature T to unity and A and B are two constants. Note that we have included the factor $2D_t$, as defined in [9], in A above since D_t remained constant in the simulation. We obtain the constant parameters $A = 0.893951$ and $B = 1350.5$ by fitting Eq. (S5) with the data corresponding to $v_0^2/D_r = 0.5$ in Fig. 4(b) in [9] and show the behavior of Eq. (S5) along with the data of [9] in Fig. S1. Note that the theoretical analysis in [9] were done in the limit $\tau_p \to 0$. This comparison shows the consistency of our assumption.

Details for the results

We have the equations governing the most probable mosaic length scale, ℓ^*, and relaxation time τ as

$$\ell^* = \left[\frac{D}{(T-T_K)+\frac{Hf_0^2}{1+G\tau_p}}\right]^{2/d} \tag{S6}$$

$$\ln\left[\frac{\tau}{\tau_0}\right] = \frac{E}{(T-T_K)+\frac{Hf_0^2}{1+G\tau_p}}. \tag{S7}$$

After setting different system-dependent constants D, E, T_K, H and G in Eq. (S6) and (S7) to unity, we obtain in $3d$

$$\ell^* = \left[\frac{1}{T-1+v_0^2/(1+\tau_p)}\right]^{2/3} \tag{S8a}$$

$$\text{and}\quad \ln\left(\frac{\tau}{\tau_0}\right) = \frac{1}{T-1+v_0^2/(1+\tau_p)} \tag{S8b}$$

When activity is controlled through f_0 keeping τ_p constant, we obtain the results in Fig. 2.

To compare with simulation data, we obtain the data from Fig. 8 of Ref. [30] and write Eq. (S7) as

$$\ln(\tau/\tau_0) = D/[(T-T_K)+\frac{f_0^2}{\Lambda}] \tag{S9}$$

and obtain different constants through fitting the above equation with a particular data corresponding to $f_0 = 1.5$. In principle, we could also obtain these parameters from the detailed microscopic knowledge of the system that we didn't attempt here. The excellent agreement between the theoretical predictions and simulation data shows that our theory captures the basic physics of the system. We also tried different forms for $\gamma_A = f(v_0, \tau_p)$. When we considered the amplitude of γ_A to be small, the detailed form of $f(v_0, \tau_p)$ didn't alter the results qualitatively which is expected from Eq. (4). We obtained the best fit with a vanishing γ_A as shown in Fig. 2 (c) and (d). It is possible that γ_A has a non-trivial dependence on activity, but it is sub-dominant for the model we considered such that it doesn't play a major role in the glassy properties of the system.

To look at the glassy behavior of an active system when activity is controlled through τ_p, we keep f_0 constant and obtain ℓ^* and τ for different τ_p from Eqs. (S8) as presented in Fig. 3 (a) and (b).

For a quantitative comparison with simulation data, we compare our theory with Ref. [28], which considers an athermal system of self-propelled particles where the dynamics of the system solely comes from activity. For this purpose we first obtain T_{eff} in terms of the parameters of our theory. The active force in the simulation of [28] obeys

$$\tau_p \dot{f}(t) = -f(t) + \eta \tag{S10}$$

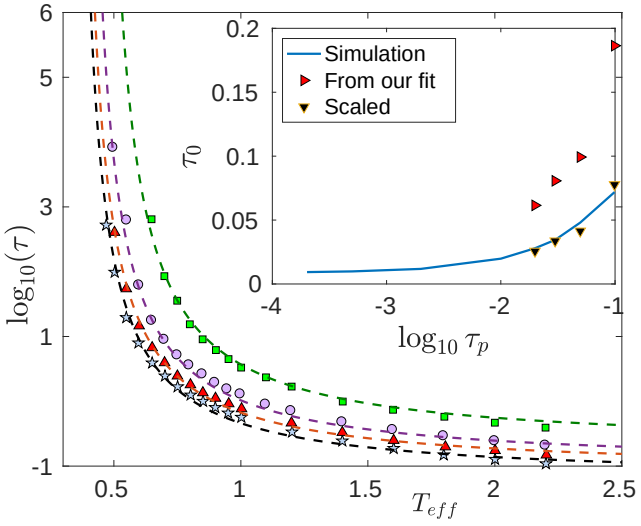

FIG. S2: Relaxation time τ as a function of T_{eff}. Data obtained from Ref. [28] and the dotted lines are plots of Eq. (S13) neglecting the second-order term in τ_p in the denominator with $\tilde{E} = 1.255$, $\tilde{T}_K = 0.305$, $\tilde{A} = 3.801$ and $\tau_0(\tau_p) = 0.0615$, 0.0807, 0.0992 and 0.1863 for $\tau_p = 0.02$, 0.03, 0.05 ans 0.1 respectively. Symbols: $\square$: $\tau_p = 0.1$, $\bigcirc$: $\tau_p = 0.05$, $\triangle$: $\tau_p = 0.03$, $\star$: $\tau_p = 0.02$. **Inset:** Plots of τ_0 as a function of τ_p. Symbols are the values obtained by fitting the theoretical expression, Eq. (S13), with the simulation data where the scaled values are $\tau_0/2.5$. Solid line corresponds to the data in Fig. 9(a) in Ref. [28].

where η is a Gaussian white noise with zero mean and variance $\eta(t)\eta(t') = 2\xi_0 T_{eff}\delta(t-t')$ (See Eq. (2) in Ref. [28]). With this active force, we obtain, following a similar calculation as in Sec. ,

$$\langle v^2\rangle = \frac{N_m p_{on} T_{eff}}{4[\lambda(1+\tau_p\lambda)+\pi\tau_p^2\sqrt{k^3/8}]}. \tag{S11}$$

We write the above expression as

$$\langle v^2\rangle = \frac{H_0 T_{eff}}{1+\tilde{A}\tau_p+\tilde{G}\tau_p^2} \tag{S12}$$

where H_0, $\tilde{A}$ and $\tilde{G}$ are constants and using Eq. (S12) in Eq. (S7), we obtain

$$\ln\tau = \ln\tau_0 + \frac{\tilde{E}}{[-\tilde{T}_K + T_{eff}/(1+\tilde{A}\tau_p+\tilde{G}\tau_p^2)]} \tag{S13}$$

where $\tilde{E} = E/H_0$ and $\tilde{T}_K = T_K/H_0$. Since Ref. [28] considers a system where temperature doesn't play any role, we have set $T = 0$. We obtain the data for relaxation time from Fig. 6 of Ref. [28] for $\tau_p = 0.02$, 0.03, 0.05 and 0.1. Since the dynamics solely arises due to activity, τ_0 becomes a function of τ_p when τ_p dominates the dynamics. Since τ_p is not large, we neglect the second-order term in τ_p in the denominator of Eq. (S13) and through fitting we obtain $\tilde{E} = 1.255$, $\tilde{T}_K = 0.305$, and $\tilde{A} = 3.801$ and

$\tau_0(\tau_p) = 0.0615$, 0.0807, 0.0992 and 0.1863 for $\tau_p = 0.02$, 0.03, 0.05 ans 0.1 respectively. These values of τ_0 are approximately 2.5 times higher than the value of τ_0 obtained in [28] through the fitting of a different equation and a different temperature regime. As the two τ_0's are obtained from fitting two different equations and in two different regimes, it's not surprising that their absolute values are different, however, we find that they are proportional. In the inset of Fig. S2 we show τ_0 as obtained in Ref. [28] by the solid line, τ_0 obtained by our fit by $\triangleright$ and we plot these values scaled by 2.5 as shown by $\triangledown$. We show the comparison of our theory with the simulation data in Fig. S2. In the main paper, we chose to present the same plot as $\log(\tau/\tau_0)$ as a function of $1/T_{eff}$ as we wanted to emphasize the dependence of τ on τ_p in the low-temperature regime.

* Electronic address: saroj.nandi@weizmann.ac.il
† Electronic address: nir.gov@weizmann.ac.il

[1] J. Prost, F. Jülicher, and J. F. Joanny, Nat. Phys. **11**, 111 (2015).
[2] J. Ranft, M. Basan, J. Elgeti, J. F. Joanny, J. Prost, and F. Jülicher, Proc. Natl. Acad. Sci. USA **107**, 20863 (2010).
[3] S. Garcia, E. Hannezo, J. Elgeti, J. F. Joanny, P. Silberzan, and N. S. Gov, Proc. Natl. Acad. Sci. (USA) **112**, 15314 (2015).
[4] S. Ramaswamy, Annu. Rev. Condens. Matter Phys. **1**, 323 (2010).
[5] N. Gravish, G. Gold, A. Zangwill, M. A. D. Goodisman, and D. I. Goldman, Soft Matter **11**, 6552 (2015).
[6] N. Kumar, H. Soni, S. Ramaswamy, and A. K. Sood, Nat. Comm. **5**, 4688 (2014).
[7] O. Dauchot, G. Marty, and G. Biroli, Phys. Rev. Lett. **95**, 265701 (2005).
[8] U. S. Schwarz and S. A. Safran, Rev. Mod. Phys. **85**, 1327 (2013).
[9] Z. Preisler and M. Dijkstra, Soft Matter **12**, 6043 (2016).
[10] J. Tailleur and M. E. Cates, Phys. Rev. Lett. **100**, 218103 (2008).
[11] T. Speck, J. Bialké, A. M. Menzel, and H. Löwen, Phys. Rev. Lett. **112**, 218304 (2014).
[12] S. C. Takatori, W. Yan, and J. F. Brady, Phys. Rev. Lett. **113**, 028103 (2014).
[13] T. F. F. Farage, P. Krinninger, and J. M. Brader, Phys. Rev. E **91**, 042310 (2015).
[14] A. P. Solon, J. Stenhammar, R. Wittkowski, M. Kardar, Y. Kafri, M. E. Cates, and J. Tailleur, Phys. Rev. Lett. **114**, 198301 (2015).
[15] U. M. B. Marconi, C. Maggi, and S. Melchionna, Soft Matter **12**, 5727 (2016).
[16] U. M. B. Marconi, N. Gnan, M. Paoluzzi, C. Maggi, and R. D. Leonardo, Sci. Rep. **6**, 23297 (2016).
[17] É. Fodor, C. Nardini, M. E. Cates, J. Tailleur, P. Visco, and F. van Wijland, Phys. Rev. Lett. **117**, 038103 (2016).
[18] D. Loi, S. Mossa, and L. F. Cugliandolo, Soft Matter **7**, 3726 (2011).
[19] G. Szamel, Phys. Rev. E **90**, 012111 (2014).
[20] S. Wang and P. G. Wolynes, J. Chem. Phys. **135**, 051101 (2011).
[21] E. Ben-Isaac, Y. Park, G. Popescu, F. L. H. Brown, N. S. Gov, and Y. Shokef, Phys. Rev. Lett. **106**, 238103 (2011).
[22] T. Shen and P. G. Wolynes, Proc. Natl. Acad. Sci. (USA) **101**, 8547 (8547).
[23] G. S. Redner, A. Baskaran, and M. F. Hagan, Phys. Rev. E **88**, 012305 (2013).
[24] G. S. Redner, C. G. Wagner, A. Baskaran, and M. F. Hagan, Phys. Rev. Lett. **117**, 148002 (2016).
[25] J. Bialké, J. T. Siebert, H. Lwen, and T. Speck, Phys. Rev. Lett. **115**, 098301 (2015).
[26] T. E. Angelini, E. Hannezo, X. Trepat, M. Marquez, J. J. Fredberg, and D. A. Weitz, Proc. Natl. Acad. Sci. (USA) **108**, 4717 (2011).
[27] L. Berthier and J. Kurchan, Nat. Phys. **9**, 310 (2013).
[28] E. Flenner, G. Szamel, and L. Berthier, Soft Matter **12**, 7136 (2016).
[29] G. Szamel, Phys. Rev. E **93**, 012603 (2016).
[30] R. Mandal, P. J. BHuyan, M. Rao, and C. Dasgupta, Soft Matter **12**, 6268 (2016).
[31] E. Ben-Isaac, É. Fodor, P. Visco, F. van Wijland, and N. S. Gov, Phys. Rev. E **92**, 012716 (2015).
[32] P. G. Wolynes and V. Lubchenko, *Structural Glasses and Supercooled Liquids* (John Wiley and Sons, Inc., Hoboken, New Jersey, 2012).
[33] S. Wang and P. G. Wolynes, J. Chem. Phys. **138**, 12A521 (2013).